JNCS Journal of Nepal Chemical Society January 2026, Vol. 46, No. 1, 61-72
ISSN: 2091-0304 (print)
DOI: https://doi.org/10.3126/jncs.v46i1.91123
RESEARCH ARTICLE

Exploring Natural Alkaloids Berberine for Sustainable Corrosion Control: A Case Study on *Mahonia nepalensis* Extracts

Anju Kumari Das[1,2], Gayatri Maiya Koju[1,3], Maya Das [1], Nabin Karki [3#], Dipak Kumar Gupta[1#], and Amar Prasad Yadav[1, a]

[1]*Central Department of Chemistry, Tribhuvan University, 44613 Kathmandu, Nepal*

[2]*Amrit Science Campus, Tribhuvan University, 44600 Kathmandu, Nepal*

[3]*Bhaktapur Multiple Campus, Tribhuvan University, 44800 Bhaktapur, Nepal*

[a] *Currently @Rajarshi Janak University (RJU), Janakpur, Nepal*

[#] *Corresponding E-mail: deepakguptas2012@yahoo.com and nabin.karki@bkmc.tu.edu.np*

(Received: December 12, 2025, revised: January 23, 2026 accepted: January 25, 2026)

Abstract

This study examines the corrosion inhibition potential of the dichloromethane/methanol (9:1) fraction derived from *Mahonia nepalens*is extract in a corrosive medium. Remarkably, this fraction, containing only 0.192 ppm of berberine, a prominent isoquinoline alkaloid known for its biological activity, exhibited a high corrosion inhibition efficiency of 86.23%. This significant performance at such a low concentration suggests that berberine, even in trace amounts, plays a vital role in passivating the metal surface, possibly through adsorption mechanisms and the development of a protective film. The results highlight the ability of *Mahonia nepalensis as a potential* alternative source of environmentally benign corrosion inhibitors and emphasize the potency of plant-derived bioactive compounds in corrosion control. These findings also open avenues for further exploration of berberine and related phytochemicals for sustainable industrial applications.

Keywords: *Mahonia nepalensis*; Dichloromethane; Inhibition efficiency; Corrosion inhibitor; Berberine.

Introduction

Corrosion is an ordinary and spontaneous process. It destroys substantial resources of industries, buildings, railway tracks, bridges, and households. According to the study carried out by NACE 2016, the economic loss caused by corrosion is about 2.5 trillion US dollars. It is nearly 3.4% of GDP. By applying different corrosion prevention methods, about 15-35%(375-875) billion US dollars of the corrosion cost can be deduced [1–4]. Corrosion inhibitors are commonly used in industry to reduce the rate of corrosion of metals and alloys in harsh environments. Corrosion inhibitors are widely used in industry. Many of the corrosion inhibitors are synthetic chemicals, but they are expensive and very hazardous to the environment. Therefore, nontoxic, environmentally friendly corrosion inhibitors are required [5]. According to the findings, the organic compounds containing Sulphur, nitrogen, oxygen, with multiple bonds are effective corrosion inhibitors. Many organic inhibitors, such as amines, aldehydes, alkaloids, nitro and nitroso compounds, have been considered and tried as corrosion inhibitors [6–9]. Based on the reaction of inhibitors on the metal surface, potential organic inhibitors can be classified as anodic,

cathodic, or mixed types [7]. A literature survey has explained that the adsorption of molecules of phytochemicals on the surface of the metal shows the inhibitive effect [10].

Most of the best-known corrosion inhibitors are green inhibitors. Green inhibitors are environmentally friendly chemical substances derived from natural sources (e.g., plant extract, biopolymers, or biowastes. Green inhibitors form the protective layer on the metal surface, which reduces or prevents the electrochemical reactions that lead to corrosion [11].Mild steel (MS) is the most famous alloy. Because of its accessibility, affordability, ease of fabrication, and good ductile strength, it is utilised in a variety of industrial applications, including metal processing, apparatus formation, and construction. It causes corrosion when the mild steel comes in contact with an acid solution during acid cleaning, storage of acid, transportation of acid, descaling, and other chemical processes[12,13].

Several chemicals are presently employed in industry to stop or to diminish the rate of metal corrosion in acidic media. The chemicals used to prevent corrosion are toxic in nature and of high cost, so it is essential to develop eco-friendly and inexpensive inhibitors. Since 1970, a lot of investigations of alkaloids for corrosion inhibition on mild steel in H_2SO_4 and HCl media have been conducted. The majority of studies utilize crude extracts from various chunks of plants, such as leaves, seeds, bark, and stems, as corrosion inhibitors. A selection of these investigations is summarized in **Table 1.** The high-altitude Himalayan flora can be a potential source of green corrosion inhibitors. The high-altitude Himalayan flora can be a potential source of green corrosion inhibitors.Mahonia *nepalensis* (MN) is a member of the Berberidaceae family and commonly called “Jamanemandro” in Nepali. It has yellow flowers and is medium size perennial, evergreen shrub. The wood and stem of this plant are used for anti-fungal, anti-inflammatory, and antibacterial activity. These plants are mainly used for medicinal purpose i.e in the treatment of skin diseases. This plant chiefly contain alkaloid. The main alkaloids found in this plant are Berberine and protoberberine. Other alkaloids like palamatine and jatrorrhizine may also be present in small quantities [21].

Table 1: Inhibition efficiency of various parts of different plant sources.

Source	**Plants**	**Inhibition efficiency (IE)**	**Medium**	**References**
Seed	Coriandrum sativum	93%	HCl	[14]
Leaves	Verbena Officinalis	91.1%	H_2SO_4	[15]
Bark	Tinospora cordifolia	93.09%	HCl	[16]
Leaves	Falcaria vulgaris	91.3%	HCl	[17]
Bark	Datura metel plant	85.73%	H_2SO_4	[18]
Fruit and peel	Praecitrullus fistulosus	87.59 %	HCl.	[9]
Flower	Rheum Ribes (Işgın)	98.4%	HCl	[7]
Fruit green husk	Walnut	95%	HCl	[19]
Stem	Tobacco	91.1 %	HCl	[20]
Stem	Murraya koenigii	96.39%	HCl	[11]

On this note, methanolic extracts obtained from a variety of plants have been developed as effective corrosion inhibitors for a number of metals, including mild steel, aluminium,

copper, and zinc. Thus, the goal of this study is designed to explore the corrosion-inhibiting properties of DCM-methanol separated fraction of *Mahonia nepalensis* for MS in 1 M sulphuric acid solution (H_2SO_4). Berberine extraction from the DCM-Methanol fraction of *Mahonia nepalensis* has been used in this work as an efficient corrosion inhibitor. The development of eco-friendly corrosion chemical inhibitors has been popular recently. Several natural products are biodegradable, nontoxic, easily available, and plentiful. Various researcher has worked on seed, flowers, leaves, bark, fruits, etc. Plant extract containing alkaloids, flavonoids, polyphenolic compounds, terpenoids, saponin and tannins as an effective corrosion inhibitor. This study aims to determine the effectiveness of alkaloids derived from the plant's bark extract for MS corrosion inhibition in an acidic environment.

In this regard, the current work examines the corrosion-inhibiting potential of berberine and its derivative, alkaloids separated from the DCM-Methanol fraction of MN. The *Mahonia nepalensis* is a medicinal plant renowned for its diverse bioactive compounds, but its application in corrosion inhibition has remained unexplored. Berberine, in particular, however, its physiochemical properties suggest it could serve as a potent corrosion inhibitor.

The novelty of this work lies in isolating berberine from *Mahonia nepalensis* (MN) and evaluating its corrosion inhibition efficacy using experimental and theoretical methods. This innovative approach aligns with growing demands for sustainable solutions in metal protection. The findings of this study are anticipated to contribute not only to the field of green chemistry but also to the advancement of cost-effective and naturally benign corrosion inhibitors.

Materials and Methods

Materials

Mahonia nepalensis (MN) bark was amassed from Lalitpur, Nepal (Latitude:27◦60′15.63″;Longitude:85◦36′52.96′). The barks were cleaned, allowed to dry in the shadow about a month, and then crushed. In order to eliminate the green pigment, the powdered MN was mixed with hexane for a whole day before being filtered. For a week, the residue was mixed with methanol for maceration. After a week, the filtrate was filtered and acidified with tartaric acid (pH 5; 3%), followed by the addition of base NH_4OH to raise the pH to 10. Dichloromethane (DCM) in a predetermined amount was added to the methanolic extract in a separating funnel. After mixing the solution in a separating flask, two distinct layers are visible. The aqueous layers were at the top, whereas the organic layers were at the bottom. The organic layer was removed carefully and placed in a rotator evaporator. The aqueous layer was collected and placed in a water bath for dryness. The greatest yield was achieved by repeating the procedure three times.

Separation of Alkaloids by Column Chromatography

1 g of organic extract of MN was taken and dissolved in 40 mL of methanol, and subjected to column chromatography. The column, having dimensions of 60 cm in length and 3 cm in diameter, was filled with 150 mg of activated silica gel (60–120) mesh. About 40.5cm of the column was eluted with hexane by using DCM-Methanol solvent media in the ratio of 9:1to 1:1. The compound was separated as shown in Figure 1. The portions were marked as M18 to M29. The nine fractions were prepared. M19 fraction was acquired by dissolving 18 mL DCM and 2 mL methanol.

Figure 1: Separation of berberine by using DCM-Methanol fraction

The subsequent compound was a brown amorphous solid, which showed an orange spot on TLC upon spraying with Dragendorff reagent, confirming the presence of an alkaloid. Electrochemical tests were performed by polarization and the electrochemical impedance method(EIS) [22]. The fractions were characterized by various methods like Fourier Transform Infrared (FTIR) spectroscopy, Ultraviolet Visible spectroscopy (UV–Vis), Raman spectroscopy, Liquid Column Mass spectroscopy (LC-MS), Scanning Electron Microscope (SEM), and Energy Dispersive X-ray (EDX).

MS Sample Preparation

For the surface analysis, a mild steel plate with dimensions of 30 x 30 x 1.6 mm was utilized, whereas a circular sample with a working area of 1 cm^2 was used for electrochemical measurement. The element composition determination revealed that the sample contained phosphorus (0.04%), sulphur (0.04%), manganese (0.8%), silicon (0.40%), carbon (0.17%), and iron. Before being used, the samples were washed with deionized water and acetone and subjected to a 15-minute ultrasonication in hexane. All samples were polished using abrasive paper of different grades (#100–1000). A blower was used to dry the sample. Once more, silicon carbide sheets graded #1200–2000 were used to abrade the sample. The samples were then dried and stored in desiccators after being sonicated with ethanol for 20 minutes. The polishing protocol was strictly maintained throughout the experiment.

Characterization of DCM-Methanol fraction

Raman Spectroscopy

The Raman spectra of the separated compounds from the DCM-Methanol fraction (M19) were recorded using a Renishaw confocal Raman microscope equipped with several lasers to confirm the various functional groups.

Fourier Transform Infrared (FTIR) Spectroscopy

ATR-FTIR analysis was done by Fourier transform infrared (PerkinElmer 10.6.2 branded instrument spectrophotometer). The spectra were measured from wavelength 4000 to 500 cm^{-1} at a resolution of 4 cm^{-1}. The compound obtained by the DCM-methanol fraction was dissolved in methanol. The sample was kept in 2.0ml quartz cuvette of 1.0cm path length. The spectra obtained show the presence of a functional group in the fraction.

Ultra-Visible Spectroscopy

The absorbance spectra of the sample were recorded using UV visible spectrometer (Labtronics 2802) in the range of 200-800nm. Quartz cuvettes with a path length of 1cm were used for all measurements. A reference sample was methanol and set to zero before measurement. The sample obtained from DCM-Methanol was dissolved in methanol and scanned. All the experiments were performed at room temperature.

Liquid Column Mass Spectroscopy (LC-MS)

LC–MS analyses were performed using a Shimadzu Prominence HPLC (LC 20AD) with a single quadrupole detector. (LCMS 2020) were used for data acquisition and processing. In order to quantify berberine, the sample was observed in SIM mode for a mass-to-charge (m/z) value of 336. Version 5.98SP1 of the lab

solution was utilized. The chromatographic separation was performed using an ACE C18 column (100 × 2.1 mm, 1.8 µm, Advanced Chromatography Technologies, USA). Under gradient elution, the mobile phase was made up of A (0.1% formic acid in water) and B (methanol). A sample of 0.5 µL was injected. The sample flow rate was 0.2 milliliters per minute. The column's temperature was maintained at 40°C. The following features of the ESI source were optimized: Nebulizing gas flow was1.5 L/min, the dissolve line temperature was 250 °C, the drying gas flow was 11 L min 1, and the heat block temperature was 350 °C.LC–MS was performed in selected-ion monitoring (SIM) mode using target ions at M+ m/z 336.1 for berberine [23].

Plant extracts are considered to contain natural compounds, including organic compounds. These compounds are isolated using standard protocols. Different types of phytochemicals are present in various parts of the plant, which encourages researchers to investigate plant extracts as effective green corrosion inhibitors. The organic layer of the Mahonia nepalensis extract contains alkaloids, as confirmed by the Mayer, Wagner, and Dragendorff tests. The surface of mild steel coated with the compound obtained from DCM-Methanol was examined by Scanning Electron Microscopy (SEM) and Energy-Dispersive X-ray Spectroscopy (EDX) to identify the elemental composition.

Corrosion Test by Electrochemical Measurements

Potentiodynamic Polarization (PDP)

Open circuit potential (OCP)of the prepared MS sample immersed in the compound obtained by DCM-Methanol fraction was measured for 30 minutes before each polarization. All the measurements were carried out as three electrode system. A platinum wire was used as the counter electrode, and a saturated calomel electrode (SCE) was employed as the reference electrode. The MS sample with an exposed surface area of 0.608 cm^2 was applied as the working electrode. Electrochemical experiments were carried out using a Gamry potentiostat (Reference 600) controlled by Gamry framework software.

Potentiodynamic polarization was performed between the anodic and cathodic limits (± 0.3 V) against OCP with a scan rate of 1 mV/s. The Tafel plot was plotted, which allowed for determining the corrosion current density (i_{corr}) and corrosion potential (E_{corr}). The Tafel slopes (ba and bc) represent the slope of the linear region and the corrosion current and corrosion potential. The following formula was used to determine the inhibitor efficiency:

$$\text{I. E.} = \frac{i^0_{corr} - i_{corr}}{i^0_{corr}} \times 100 \qquad (1)$$

i_{corr} and i^0_{corr} are corrosion current densities in an acid-containing inhibitor solution and only acid, respectively [24,25].

Electrochemical Impedance Spectroscopy (EIS)

The separated fraction of DCM-methanol was employed to measure electrochemical impedance on a Gamry Potentiostat. The EIS was performed with a 1 mV s-1 scan rate. The frequency range was set to 100000 Hz to 0.01 Hz, and the AC signal was 10 mv. After the analysis was completed, Z-view software was used to fit the EIS data with many equivalent electrical circuit models in order to produce parameters like charge transfer resistance (Rct) and constant phase element (CPE) values. The % IE was computed using equation (2).

$$\text{IE}(\eta) = \frac{R_{P-R^0_P}}{R_p} \times 100 \qquad (2)$$

Rp and Rp^0 are the polarization resistances in acid-containing inhibitors and acid, respectively.

Results and Discussion

Raman Spectra

Figure 2 represents the Raman spectra of the separated fraction of *Mahonia nepalensis* (MN). The whole range from 720 to 1700 cm^{-1} is characterized by in-plane vibrations. The modes corresponding to C–H bond vibrations

with weak displacements of other atoms, primarily C, characterize the high-frequency range of 3000–3300 cm^{-1}. The peaks occur in the ranges 1275 cm^{-1} corresponds to C-N stretching skeletal vibrations, typical for alkaloids and other phenolic compounds. The peak also occurs in the range1727cm^{-1} shows C=O vibrations (carbonyl stretching), which is typically strong in this region indicate the presence of a carbonyl-type functional group.

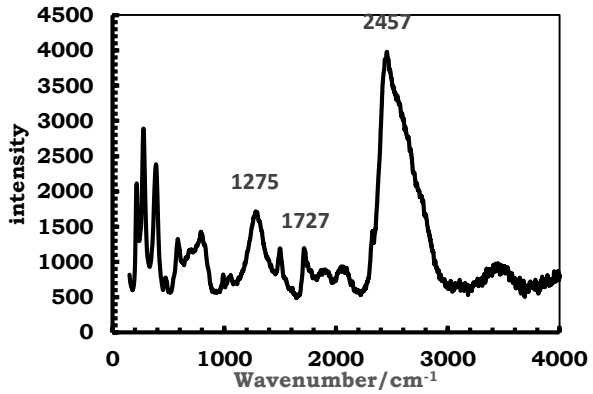

Figure 2: Raman spectra of the separated fraction of *Mahonia Nepalensis*

UV–visible spectra

Figure 3 shows the UV- visible spectra of the separated fraction, revealing a strong peak at around 305 nm, and a relatively weak one at about 395 nm. The absorption peak at 305nm with an absorbance of approximately 0.27, suggesting a strong $\pi \rightarrow \pi *$transition, which is typical for aromatic or conjugated systems. A smaller peak at 395nm, possibly indicating an n→ $\pi *$transition or *the* presence of extended conjugation. The spectrum covers the range from 200 nm to 800 nm, although absorbance becomes negligible after about 450nm. This UV-Vis profile might be consistent with compounds like berberine or Jatrorrhizine, both of which shows cha3.2racteristics absorbance in the UV-range due to a conjugated structure [26].

Fourier Transform Infrared (FTIR) spectra

The FTIR spectra of the separated fraction containing the compound are shown in **Figure 4**. The significant peak at 3338 cm^{-1} resembles the stretching vibrations of – OH. The peak at 2947cm^{-1} is assigned to the C-H bond. The peak at 2850 cm^{-1} resembles with the stretching vibration of N-H of alkaloids. The significant peaks at about 2000 cm^{-1}, 1776 cm^{-1}, and 1550 cm^{-1}correspond to the stretching vibrations of C=C, C=O, and N-O of nitro compounds, respectively. These peaks of functional groups of separated compounds are similar to those of the berberine. In the existing study, the result of FTIR spectra was used to support the condition that corrosion inhibition of mild steel in acid media is because of the adsorption of inhibitor molecules [27,28] .

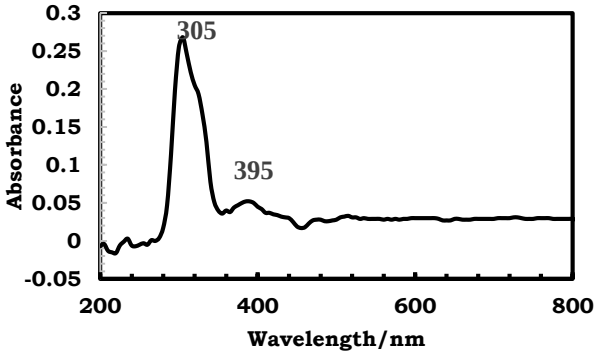

Figure 3: UV -Visible of Separated fraction

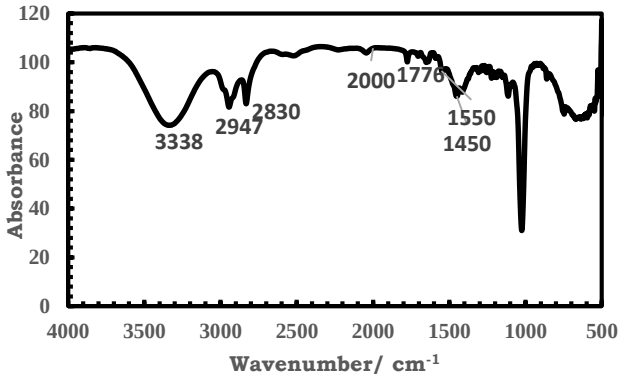

Figure 4: FTIR of the separated fraction

Table 2: Separated M19 fraction with concentration of berberine

Sample	Retention time	Concentration of berberine (ppm)
Fraction M19	19.927	0.192

Liquid Column Mass Spectroscopy (LC-MS)

Figure 5 shows the LCMS spectra of compounds present in the separated fraction.

LC-MS spectra at m/z 336.1 showed Berberine's [M]+ ions. The results confirmed that the mass of berberine in the MN extract ([M H] + (m/z 336.1) matched with the mass of standard berberine ([M H] + (m/z 336.1247)). The berberine in MN reached its highest peak at a retention time of 19.927 minutes. The MS/MS chromatogram showed similar fragmentation patterns for the reference berberine and the compound from the MN extract. Among the several fractions produced, the DCM-Methanol fraction of the MN extract contains 0.192 ppm of berberine.

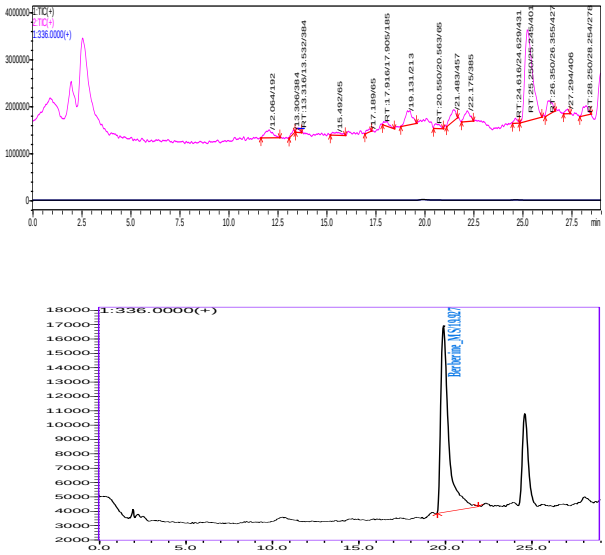

Figure 5: Extracted ion chromatogram of sample number M19 $[M+H]^+$=336

Open Circuit Potential

Figure 7 shows the open-circuit potential (OCP) measured over 30 minutes after a 24-hour immersion of MS in acid and inhibitor solutions. The OCP vs time plots are straight lines, indicating the development of a steady-state potential in both cases. The straight lines also indicate the complete removal of the iron oxide layers and the formation of an inhibitive or protective layer on the metal surface by the DCM-Methanol fraction of MN. Additionally, the results show that the addition of an inhibitor does not shift the open-circuit potential in the cathodic (negative) direction by more than 85 mv. This result indicates that the M19 fraction acts as a mixed inhibitor and adsorbs quickly, forming a protective layer on the metal surface through the adsorption of active compounds (alkaloids).

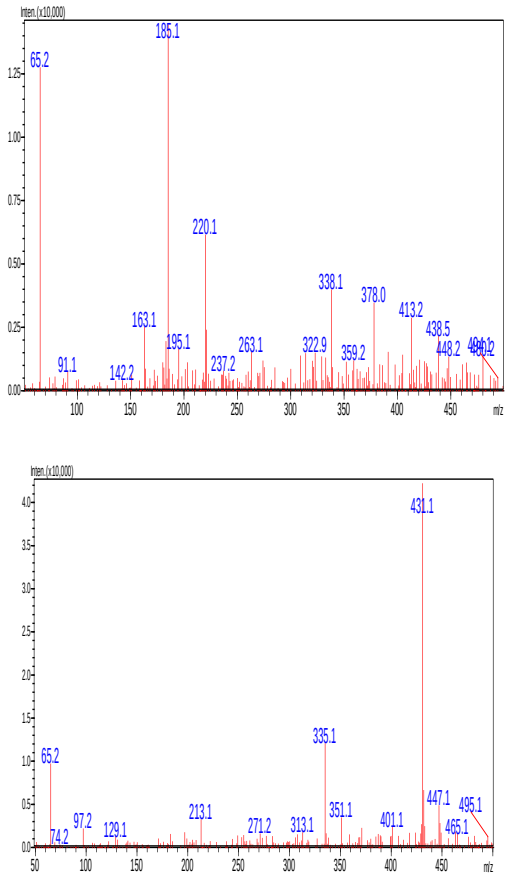

Figure 6: Molecular ion mass spectra of M + H]+ ions

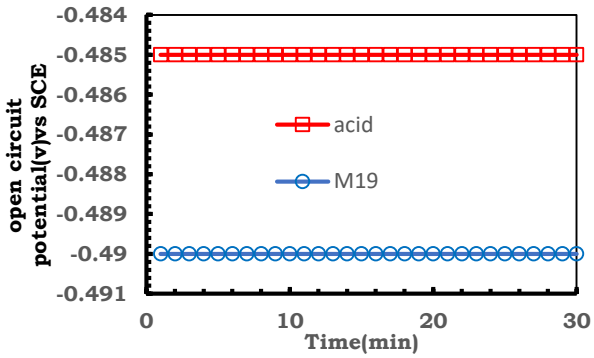

Figure 7: Open-circuit potential of MS in 1 M H_2SO_4 and the M19 fraction

Potentiodynamic Polarization Measurements

Potentiodynamic polarization investigations were carried out to examine the inhibitor's behavior towards the anodic and cathodic processes. **Table 3** represents the polarization indices of the inhibitor. **Figure 8**

shows the cathodic and anodic polarization curves for metallic dissolution in 1 M H_2SO_4 and inhibitor solution. The cathodic and anodic reactions and processes were affected by the DCM Methanol fraction of *Mahonia nepalensis*, resulting in a notable decrease in the corrosion current density (i_{corr}) without altering the Tafel curve.

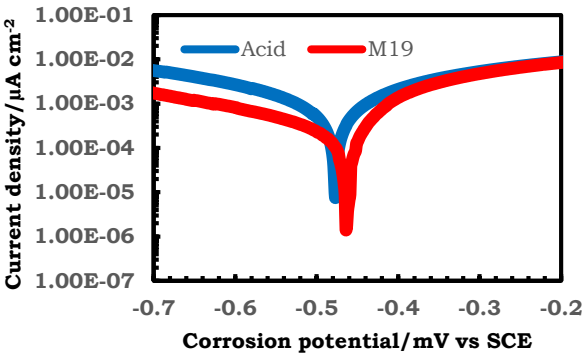

Figure 8: PDP curves of MS in 1 M H_2SO_4 and inhibitor solution

The current density is significantly lower for the M19 fraction than for acid alone, indicating a reduced corrosion rate. Cathodic and anodic branches are both suppressed, suggesting M19 acts as a mixed-type inhibitor. The decline in current density confirms that M19 exhibits higher inhibition efficiency even at low alkaloid concentrations.

Table 3: Potentiodynamic polarization parameters of MS in M19 fractions

Sample	Ba (V/decade)	Bc (V/decade)	i_{corr} (μA/cm²)	E_{corr} (mV)	I.E.%
Acid	0.029	- 0.066	1.70E-04	0.471	
M19	0.026	- 0.058	4. 56E-5	0.457	73.17

Electrochemical impedance spectroscopy (EIS)

The expression $ZCPE=1/Q(jW)^n$ represents the impedance function of CPE, where Q is the CPE's magnitude, j is the imaginary number ($j2 = -1$), w is the angular frequency ($w = 2\pi f$), and n is the CPE exponent ($-1 \leq n \leq +1$), which can be used to measure the surface's unevenness.

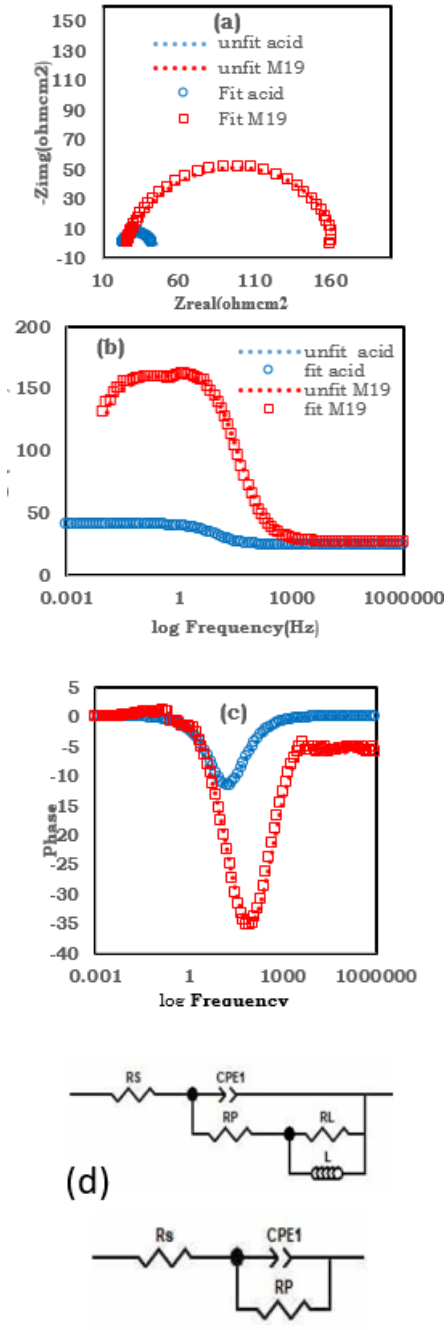

Figure 9: a) Nyquist plots (b) Bode plot (c) Bode plot of Phase angle (d) Equivalent electrical circuit model for mild steel dipped in M19 fraction

For the acid and inhibitor solutions at low concentrations, the Nyquist plots reveal a small capacitive semicircle in the high and middle-frequency areas. This part of the acid solution consists of accumulation resistance resulting from the barrier effect of corrosion products at the MS/H_2S0_4 solution interface (Ra), diffuse layer resistance (Rd), and charge transfer resistance at the metal/solution interface

(Rct).The resistance of the protective film formed by the adsorbed molecules on the metal surface and the potential build-up of metal-organic complexes (Rf) are also present in the inhibited solution. At low frequencies, a second inductive loop emerged. This loop is typically taken into account by relaxation processes on the MS surface or insoluble and unstable corrosion products at the MS/solution interface. This capacitive loop's diameter, which correlates to Rp, shows that more extract molecules have been adsorbed, improving the surface film's protective qualities. The increase in the value of R_p shows the adsorption of the inhibitor[29–31]. When the inhibitor solution was used, the CPE values decreased. These findings suggest that components of alkaloids attach to the MS surface, improving protection and inhibitor adsorption rates. The decrease in CPE values also suggests that more deposited inhibitor molecules have been replaced by previously adsorbed water molecules, which lowers the ratio of the uncovered MS surface and either raises the thickness of the protective layer at the MS/H_2SO_4 solution interface or increases surface coverage according to the Helmholtz model:

$$C=\frac{\varepsilon 0 \varepsilon s}{d} \qquad (3)$$

Here, S and d represent the surface area of MS and the thickness of the inhibitor at the metal/solution interface. ε^0 and ε are the dielectric constants of the vacuum and corrosive medium, respectively.

Table 4: Electrochemical impedance data of MS in 1.0 M H_2SO_4, with M19.

Sample	CPE (10^{-5} /s ^{n} Ω^{-1} cm^{-2})	N	Rp (Ω cm^2)	L (H)	R_L (Ω cm^2)	η %
Acid	133.82	0.8749	15.8			
M19	10.757	0.81502	114.8	10	24.91	86.23

The value of n is almost constant. The value of n somewhat decreases when an inhibitor is present. The presence of inhibitor molecules, corrosion products, or metal-inhibitor complexes on the metal surfaces causes this reduction. ZView Software was used to fit and analyze the impedance data. The results are displayed in the table 4.

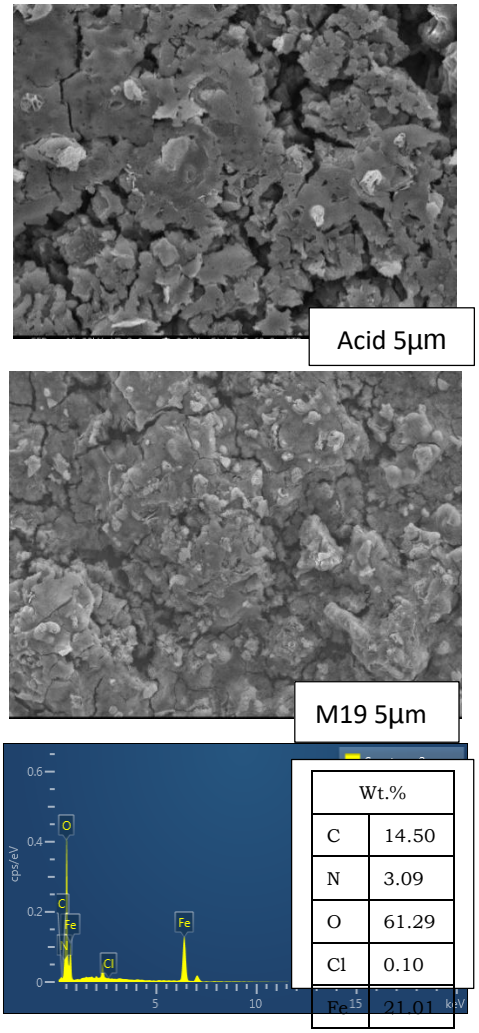

Figure 10: SEM and EDX of mild steel, M19 fraction after 24-hour immersion

Surface Analysis

The SEM with EDX of an MS dipped in 1 M H_2SO_4 and inhibitor DCM-Methanol fraction of MN is displayed in **Figure 10**. The MS sample submerged in a 1 M H_2SO_4 solution showed a rough surface and was severely damaged due to corrosion. However, MS immersed in DCM-Methanol fraction of MN extract (M19) for 24 hours showed less uneven and surface damage, indicating the formation of a protective inhibitor film at the mild steel surface.The MS surface is smoother and more compact in the DCM-Methanol fraction of MN extract than in the acid solution [26]. The elements C, N, O, and Fe were visible in the EDX spectra as shown in Figure 10. The extract contains alkaloids that adsorb heteroatoms (N, O) and aromatic rings on the metal surface. The preventive barrier formed by adsorption prevents additional interactions between metal surfaces and acidic environments.

Conclusions

The DCM–methanol extract (9:1 ratio) derived from *Mahonia nepalensis* bark, enriched with berberine, exhibits outstanding corrosion inhibition for mild steel in 1 M H_2SO_4. This fraction achieves an inhibition efficiency exceeding 86% at room temperature with only 0.192 ppm of berberine, highlighting its potential as a low-cost and effective industrial corrosion inhibitor. Potentiodynamic polarization results indicate a noticeable reduction in cathodic current density, suggesting diminished hydrogen gas evolution without modifying the underlying reaction mechanism. Analysis of polarization behaviour and open circuit potential (OCP) confirms the inhibitor's mixed-mode activity. Electrochemical impedance spectroscopy (EIS) results show a decline in double-layer capacitance along with an increase in polarization resistance, supporting the mixed inhibition mechanism. Additionally, surface analysis using SEM and EDX confirms the adsorption of inhibitor molecules on the MS surface, forming a preventive barrier layer.

Acknowledgements

A.K. Das gratefully acknowledges the University Grants Commission (UGC), Sanothimi, Nepal, for the Ph.D. funding support (UGC Award No: PhD-75/76S&T-3). The authors also extend their appreciation to the Council of Scientific and Industrial Research (CSIR) – Institute of Minerals and Materials Technology (IMMT), Bhubaneswar, India, for conducting SEM-EDX analysis. Sincere thanks are also due to the National Food & Feed Reference Laboratory (NFFRL), Department of Food Technology and Quality Control (DFTQC), Kathmandu, Nepal, for facilitating LC-MS analysis.

Author's contribution statement

A. K. Das: Writing – original draft, Investigation, Formal analysis, Data curation. **G. M. Koju:** Investigation and Data curation. **M. Das:** Formal analysis and Data curation. **N. Karki:** Writing – review & editing, Supervision, Project administration. **D. K. Gupta:** Writing – review & editing, Supervision, Formal analysis. **A. P. Yadav:** Writing – review & editing, Supervision, Conceptualization.

Conflicts of Interest

The authors state that they have no competing interests in this work.

Data Availability Statement

The data presented in this study are available upon request from the corresponding authors.

References

1. G. Koch, J. Varney, O. Moghissi and M. Gould, *NACE International Report*, NACE International, 2016.
2. G. H. Koch, M. P. H. Brongers, N. G. Thompson, Y. P. Virmani and J. H. Payer, Cost of corrosion in the United States, in *Handbook of Environmental Degradation of Materials*, Elsevier, 2005, pp. 3–24.
3. J. Richardson and J. Dawson, Economic aspects of corrosion, *Corrosion*, 2010, 66, 3040–3051.

4. C. Verma, E. E. Ebenso, I. Bahadur and M. A. Quraishi, An overview on plant extracts as environmentally sustainable and green corrosion inhibitors for metals and alloys in aggressive corrosive media, *Journal of Molecular Liquid*, 2018, 266, 577–590.
5. G. Palanisamy, Corrosion inhibitors, in *Corrosion Inhibitors*, ed. A. Singh, IntechOpen, 2019
6. M. A. Ameer and A. M. Fekry, Corrosion inhibition of mild steel by natural product compound, *Progress in Organic Coating*, 2011, 71, 343–349.
7. F. Kaya, R. Solmaz and İ. H. Geçibesler, Methanol extract of *Rheum ribes* flower as a natural corrosion inhibitor for mild steel in 1 M HCl solution, *Journal of Industrial and Engineering Chemistry*, 2023, 122, 102–117.
8. A. Khadraoui, A. Khelifa, K. Hachama and R. Mehdaoui, *Thymus algeriensis* extract as eco-friendly corrosion inhibitor for aluminium alloy in 1 M HCl medium, *Journal of Molecular Liquid*, 2016, 214, 293–297.
9. A. Kumar and C. Das, Corrosion inhibition of mild steel by *Praecitrullus fistulosus* extracts, *Science of the Total Environment*, 2024, 929, 172569.
10. A. Kumari, N. Kaur, M. Kaur, F. M. Husain, P. K. Bhowmik and H. S. Sohal, Sustainable corrosion prevention of mild steel in acidic media using *Rumex nepalensis* extract, *RSC Advance*, 2025, 15, 924–937.
11. B. Pandey, D. Pandey, N. P. Pant, D. P. Bhattarai, M. Dhakal and H. B. Oli, Methanol extract of *Murraya koenigii* stem as green corrosion inhibitor for mild steel in 1 M HCl solution, *Results in Surfaces and Interfaces,* 2024, 16, 100245.
12. B. Li, W. Wang, L. Chen, X. Zheng, M. Gong, J. Fan *et al.*, Magnolia grandiflora leaves extract as corrosion inhibitor for mild steel in acid solution, *International Journal of Electrochemical Science*, 2023, 18, 100082.
13. Z. Sanaei, M. Ramezanzadeh, G. Bahlakeh and B. Ramezanzadeh, Rosa canina fruit extract as green corrosion inhibitor for mild steel in 1 M HCl solution, *Journal of Industrial and Engineering Chemistry*, 2019, 69, 18–31.
14. L. Kadiri, M. Galai, A. Ouass, Y. Essaadaoui, M. Khattabi, S. Kaya *et al.*, Performance of *Coriandrum sativum* extract as corrosion inhibitor for mild steel in phosphoric acid medium, *International Journal of Electrochemical Science*, 2024, 19, 100825.
15. A. E.-A. S. Fouda, A. F. Molouk, M. F. Atia, A. El-Hossiany and M. S. Almahdy, *Verbena officinalis* leaf extract as anti-corrosion inhibitor for carbon steel in acidic environment, *Scientific Reports*, 2024, 14, 16112.
16. A. Phuyal, M. Poudel, R. Bhandari, S. Budhathoki, D. Baral, A. Bhattarai *et al.*, Phytochemical composition and corrosion inhibitory efficiency of plant extracts on mild steel, *Butwal Campus Journal*, 2024, 7, 25–40.
17. M. Alimohammadi, M. Ghaderi, S. A. A. Ramazani and M. Mahdavian, *Falcaria vulgaris* leaves extract as eco-friendly corrosion inhibitor for mild steel in hydrochloric acid media, *Scientific Reports*, 2023, 13, 3737.
18. S. Mohanasundaram, S. Geetha, R. Nagajothi, VP Sundramurthy, J. Vijayakumar, NS Alharbi, M. Thiruvengadam, Evaluation of anti-corrosion potential of Datura Metel plant extract on mild steel upon sulphuric acid exposure, Canadian Metallurgical Quarterly, 2025 64(1):196-209..
19. A. R. Shahmoradi, M. Ranjbarghanei, A. A. Javidparvar, L. Guo, E. Berdimurodov and B. Ramezanzadeh, Walnut green husk extract as corrosion inhibitor for mild steel in 1 M HCl, *Journal of Molecular Liquid*, 2021, 338, 116550.
20. L. Qiu, X. Li, B. Tan, Y. Xie and S. Deng, Tobacco stem extract as corrosion inhibitor for

steel in HCl solution, *Industrial Crops and Products*, 2025, 224, 120367.

21. R. Thusa and S. Mulmi, Phytoconstituents and biological activities of *Mahonia nepalensis* and *Berberis aristata*, *Nepal Journal of Biotechnology*, 2017, 5, 5–13.
22. P. B. Raja, A. K. Qureshi, A. Abdul Rahim, H. Osman and K. Awang, *Neolamarckia cadamba* alkaloids as eco-friendly corrosion inhibitors for mild steel in 1 M HCl, *Corrosion. Science*, 2013, 69, 292–301.
23. W. Hua, L. Ding, Y. Chen, B. Gong, J. He and G. Xu, Determination of berberine in human plasma by LC–ESI–MS, *Journal of Pharmaceutical and Biomedicical Analysis*, 2007, 44, 931–937.
24. N. Hossain, M. A. Chowdhury, M. Rana, M. Hassan and S. Islam, *Terminalia arjuna* leaves extract as green corrosion inhibitor for mild steel in HCl solution, *Results in Engineering*, 2022, 14, 100438.
25. A. Kumari Das, S. Neupane, K. K. Nayak, S. Shrestha, N. Karki, D. K. Gupta *et al.*, Mahonia nepalensis fraction containing berberine as corrosion inhibitor for mild steel, *Results in Chemistry*, 2024, 12, 101866.
26. N. Karki, S. Neupane, D. K. Gupta, A. K. Das, S. Singh, G. M. Koju *et al.*, Berberine isolated from *Mahonia nepalensis* as eco-friendly corrosion inhibitor for mild steel, *Arabian Journal of Chemistry*, 2021, 14, 103423.
27. R. Karthik, P. Muthukrishnan, A. Elangovan, B. Jeyaprabha and P. Prakash, *Cassia senna* extract as green inhibitor for mild steel in hydrochloric acid, *Advances in Civil Engineering Materials*, 2014, 3, 20140010.
28. Q. H. Zhang, B. S. Hou, Y. Y. Li, G. Y. Zhu, H. F. Liu and G. A. Zhang, Chitosan derivatives as eco-friendly corrosion inhibitors for mild steel in acidic solution, *Corrosion Science.*, 2020, 164, 108346.
29. I. Arshad, K. Qureshi, A. S. Saleemi, A. Abdullah, A. A. A. Bahajjaj, S. Ali *et al.*, Melamine–isatin tris Schiff base as corrosion inhibitor for mild steel in hydrochloric acid, *RSC Advance*, 2023, 13, 19301–19311.
30. F. Kaya, R. Solmaz and İ. H. Geçibesler, Adsorption and corrosion inhibition behavior of *Rheum ribes* leaf extract on mild steel in 1 M HCl, *Journal of Taiwan Institute of Chemical Engineers,* 2023, 143, 104712.
31. A. Sharifi-Rad, J. Mehrzad, M. Darroudi, M. R. Saberi and J. Chamani, Berberine nanoemulsions: biological activities and binding mechanisms, *Journal of Biomolecular Structure and Dynamics* 2021, 39, 1029–1043.
32. R. Solmaz, A. Salcı, Y. A. Dursun and G. Kardaş, A comparative study on the adsorption and corrosion inhibition efficiency of acriflavine on mild steel in 1 M HCl, *Colloids and Surfaces A: Physicochemical and Engineering Aspects*, 2023, 674, 131908.